# Influence of the Stiffness of Testing Machines on the Adherence of Elastomers

MICHEL BARQUINS, *Equipe de Recherche de Mécanique des Surfaces du C.N.R.S., Laboratoire Central des Ponts et Chaussées, 75732 Paris Cedex 15, France*

## Synopsis

It is shown that the introduction of the fracture mechanics concepts, such as the strain energy release rate $G$, to solve the problem of the adherence of elastomers, the edge of contact being seen as a crack propagating in mode I in the interface, allows one to predict the dependence of the adherence force with the stiffness of testing machines. Moreover, it is shown the general equation of the kinetics of adherence proposed in 1978 by Maugis and Barquins, $G - w = w\phi(a_T v)$, where $w$ is Dupré's work of adhesion and $\phi$ a dissipation function characteristic of the material only depending on temperature and crack speed, is confirmed whatever the stiffness of the testing machine and the instantaneous deformation imposed on the system. Experiments realized with a hemispherical glass lens in contact on a polyurethane surface verify theoretical predictions with an accuracy better than 1%.

## INTRODUCTION

The adhesive contacts of rigid spherical punches on elastic solids have been studied by Johnson et al. (JKR theory),[1] by introducing the energy balance concept.[2] It is shown that, due to the existence of molecular attraction forces, contact area and elastic displacement are larger than values that can be deduced from the classical Hertz's theory. The energy balance theory is based on minimizing the total energy of the system at equilibrium, and the adherence force is obtained if the first derivative of the total energy takes the value zero. Maugis et al.[3] have shown that this procedure cannot give information about the stability of the system, which depends on the second derivative of the total energy. In order to solve this problem, Maugis and Barquins[4,5] have reintroduced the concepts of fracture mechanics such as the strain energy release rate $G$ and studied the stability by the sign of the derivative of $G$. So, it can be demonstrated that the stability depends on the stiffness $k_m$ of testing machines, and monotonically increases with $k_m$ when there is a change from a fixed load solicitation ($k_m = 0$) to a fixed grips solicitation ($k_m = \infty$).[6]

Moreover, the concepts of fracture mechanics have been used to study the kinetics of the adherence by the general equation[4] $G - w = w\phi(a_T v)$, where $w$ is Dupré's work of adhesion and $\phi$ a dissipation function, characteristic of the viscoelastic material and of propagation in mode I. It was shown that the knowledge of $\phi$, which depends only on the material property, the temperature, and the speed of the contact edge (seen as a crack propagating in the interface), allows one to predict the kinetics of propagation under fixed and cyclic load or fixed crosshead velocity conditions.[4,7,8]

Journal of Applied Polymer Science, Vol. 28, 2647–2657 (1983)
 CCC 0021-8995/83/082647-11$02.10

We show that theoretical predictions are also verified, with a reproducibility better than 1%, in a test at fixed displacement with a finite stiffness.

## ADHERENCE AT FIXED DISPLACEMENT Δ

Let us consider (Fig. 1) the equilibrium of a rigid sphere of radius $R$ in contact on an elastic half-space under the load $P_0$. The contact radius $a_0$ and the displacement $\delta_0$ are given by the JKR theory[1]:

$$a_0 = ((R/K)\{P_0 + 3\pi wR + [6\pi wRP_0 + (3\pi wR)^2]^{1/2}\})^{1/3} \quad (1)$$

$$\delta_0 = a_0^2/3R + 2P_0/3a_0K \quad (2)$$

where $w$ is Dupré's work of adhesion and $K$, a constant of elasticity equal to $4E/3(1 - \nu^2)$, $E$ and $\nu$ being the Young modulus and the Poisson ratio of the elastic solid, respectively.

The edge of the contact area, like any 3-dimensional crack, is subjected locally to a plane strain state, so that the strain energy release rate is linked to contact radius $a$ and displacement $\delta$ by[4]

$$G = (3K/8\pi R^2 a)(a^2 - R\delta)^2 \quad (3)$$

and the junction of the elastic solid to the sphere is vertical (fracture mechanics geometry).[9] At equilibrium, i.e., $a = a_0$ and $\delta = \delta_0$, $G$ takes the value $w$ (Griffith criterion).

Starting from the equilibrium state under the load $P_0$, it is possible by turning the screw (Fig. 1) to impose on the system a fixed displacement Δ. This one is divided in elastic displacement $\delta_m$ of the spring of stiffness $k_m$ and elastic displacement $\delta$ of the solid in contact with the rigid sphere. Thus, a force $P = k_m\delta_m$ is exerted by the spring on the elastic solid and taking into account initial loading, one can write

$$\Delta = \delta + P/k_m - \delta_0 - P_0/k_m \quad (4)$$

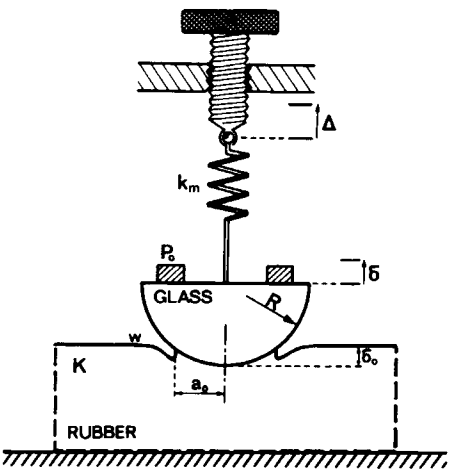


Fig. 1. Principle of the apparatus to study the state of equilibrium of a rigid sphere in contact on an elastic solid, with a testing machine with a finite stiffness.

Using the equation of state of the system[5]

$$P = (3aK/2)(\delta - a^2/3R) \tag{5}$$

similar to eq. (2) out of equilibrium, the eq. (4) becomes

$$\delta = \left(\frac{a^3K}{2Rk_m} + \Delta + \frac{P_0}{k_m} + \delta_0\right) \Big/ \left(1 + \frac{3aK}{2k_m}\right) \tag{6}$$

Introducing the reduced values[1]

$$\|P\| = P/3\pi wR$$

$$\|a\| = \frac{a}{(3\pi wR^2/K)^{1/3}}$$

$$\|\delta\| = \frac{\delta}{(\pi^2w^2R/3K^2)^{1/3}}$$

and adding

$$\|\Delta\| = \frac{\Delta}{(\pi^2w^2R/3K^2)^{1/3}}$$

and

$$\|k_m\| = \frac{k_m}{(3a_0K/2)}$$

the stiffness of the spring being normalized by the stiffness of the initial contact, eq. (6) can be rewritten as

$$\|\delta\| = \left[\frac{\|a\|^3}{\|a_0\| \cdot \|k_m\|} + \|\Delta\| + \|a_0\|^2 + \frac{2\|P_0\|}{\|a_0\|}\left(1 + \frac{1}{\|k_m\|}\right)\right] \Big/ \left(1 + \frac{\|a\|}{\|a_0\| \cdot \|k_m\|}\right) \tag{7}$$

with

$$\|a_0\|^3 = \|P_0\| + 1 + (2\|P_0\| + 1)^{1/2}$$

Equilibrium at fixed $\Delta$ is given by $G = w$, i.e.,

$$\|G\| = \frac{(3\|a\|^2 - \|\delta\|)^2}{8\|a\|} = 1 \tag{8}$$

and the limit of stability by[5]

$$\left(\frac{\partial\|G\|}{\partial\|a\|}\right)_{\|\Delta\|} = \left(\frac{\partial\|G\|}{\partial\|a\|}\right)_{\|\delta\|} + \left(\frac{\partial\|G\|}{\partial\|\delta\|}\right)_{\|a\|} \cdot \left(\frac{\partial\|\delta\|}{\partial\|a\|}\right)_{\|\Delta\|} = 0 \tag{9}$$

The locus of equilibrium points is represented in reduced coordinates by the curve $\delta(a)$ in Figure 2. For comparison, the case of a nonadhesive contact is drawn (curve $\delta_H$, Hertz's theory). Curves $(\delta)_\Delta$ show the variation of $\|\delta\|$ with $\|a\|$ at fixed displacement $\|\Delta\|$; these are independent of Dupré's work of adhesion, and their minima, when they exist, are all located on Hertz's curve $\delta_H$. Moreover, these curves intersect the $\delta$-axis for finite values of $\delta$ (as point $Q'$) simply related to $\|\Delta\|$ by

$$\|\delta\|_{a=0} = \|\Delta\| + \|a_0\|^2 + (2\|P_0\|/\|a_0\|)(1 + 1/\|k_m\|) \tag{10}$$

The radius of contact corresponding to the limit of stability can be deduced

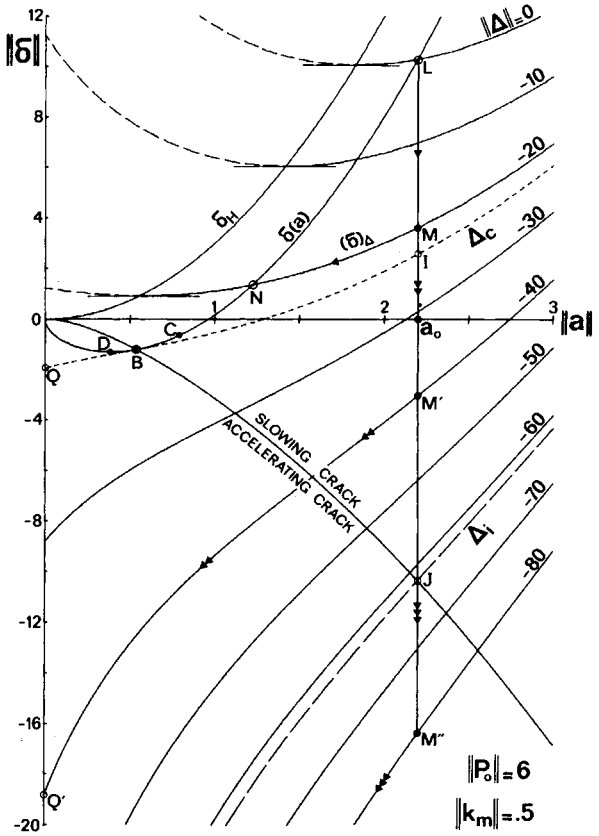


Fig. 2. Relations between elastic displacement $\delta$ and radius of contact area $a$ of a rigid sphere in contact on an elastic body, in reduced coordinates. The equilibrium curve is $\delta(a)$; curves $(\delta)_\Delta$ show the variation of $\delta$ with $a$ at constant displacement $\Delta$. The curve $\delta_H$ is given by the Hertz's theory.

from eqs. (8) and (9); its value $\|a_c\|$ is solution of the equation

$$\frac{2\|a\|^5}{\|k_m\|^2} + \frac{4\|a_0\| \cdot \|a\|^4}{\|k_m\|} + 2\|a_0\|^2 \cdot \|a\|^3 - \frac{\|a\|^2}{\|k_m\|^2} - \frac{2\|a_0\| \cdot \|a\|}{3\|k_m\|} - \frac{\|a_0\|^2}{9} = 0 \tag{11}$$

and is represented by the point $B$ in Figure 2. As expected, eq. (11) gives with $k_m = 0$ and $k_m = \infty$ the classical values for a test at fixed load (point $C$, $\|a\|^3 = 1/2$) and at fixed grips condition (point $D$, $\|a\|^3 = 1/18$), respectively.[1,4]

The corresponding value of $\|\delta_c\|$ can be deduced from eq. (8):

$$\|\delta_c\| = -9\|a_c\|^2 \left(1 + \frac{\|a_c\|}{3\|a_0\| \cdot \|k_m\|}\right) \Big/ \left(1 + \frac{3\|a_c\|}{\|a_0\| \cdot \|k_m\|}\right) \tag{12}$$

Hence, the critical value of $\|\Delta\|$ to observe a stable equilibrium is equal to

$$\|\Delta_c\| = -3\|a_c\|^2 \left(3 + \frac{13\|a_c\|}{3\|a_0\| \cdot \|k_m\|} + \frac{2\|a_c\|^2}{\|a_0\|^2 \cdot \|k_m\|^2}\right) \Big/ \left(1 + \frac{3\|a_c\|}{\|a_0\| \cdot \|k_m\|}\right) - \|a_0\|^2 - \frac{2\|P_0\|}{\|a_0\|}\left(1 + \frac{1}{\|k_m\|}\right) \tag{13}$$

The variation of $\|\delta\|$ with $\|a\|$ at constant $\|\Delta_c\|$ is plotted in Figure 2 (dotted line). Obviously, the equilibrium curve $\delta(a)$ and the limit curve $(\delta)_{\Delta_c}$ are tangent at the point $B$.

## CRACK PROPAGATION AT FIXED DISPLACEMENT $\Delta$

The equilibrium defined by $G = w$ may be disrupted by a change in displacement $\Delta$. When $G > w$, the two solids, elastic body and rigid sphere, begin to separate and the contact area decreases; conversely, if $G < w$, the contact area increases and the crack recedes. The difference $G - w$ represents the force applied per unit length of crack; it is the "motive" of the crack, which takes a limiting speed $v$ that depends on the temperature. If it is assumed that viscoelastic losses are proportional to $w$,[10,11] and localized at the crack tip, one can write[4]

$$G - w = w\phi(a_T v) \tag{14}$$

where the second member corresponds to the viscous drag resulting from the losses at the crack tip ($a_T$ is the shift factor in the WLF transformation). $\phi$ is a dimensionless function of the speed of propagation and the temperature. It was shown[4,5,12] that it is independent of loading system, of the nature of the rigid material in contact, and of the geometry. The function $\phi$ is characteristic of the viscoelastic material for the propagation in mode I, quite probably directly linked to the frequency dependence of the imaginary component of the Young's modulus. Knowledge of the function $\phi$ makes it possible to predict the evolution of the contact in all circumstanccs. The prediction only assumes that the rupture is adhesive, i.e., that the crack propagates at the interface, and that viscoelastic losses are limited to the crack tip, meaning that gross displacement must be purely elastic. Moreover, the multiplicative effect of $w$ on viscoelastic losses [eq. (14)] has been confirmed by a test equivalent to $\pi/2$-peeling test, namely measurement of the rolling resistance of a glass cylinder in contact with a polyurethane surface, at various levels of relative humidity.[12,13]

Starting from the equilibrium under the load $P_0$ (point $L$ in Fig. 2), let us apply, at the time $t = 0$, an instantaneous tensile displacement $\Delta$; the equilibrium is then disrupted, the strain energy release rate [eq. (3)] increases, and the contact area decreases as the crack advances. It is shown in Figure 2 that there is first from equilibrium point $L$, an instantaneous modification of displacement $\delta$ at constant contact radius $a_0$ (branch $LM$ or $LM'$), corresponding to the elastic response of the elastomer. This is followed by a simultaneous variation of $\delta$ and $a$ at fixed displacement $\Delta$ along curve $(\delta)_\Delta$, which may lead to a new equilibrium state (branch $MN$) if $\Delta > \Delta_c$, or to rupture (branch $M'Q'$), if not. The crack propagation speed increases or decreases according to whether the sign of $(\partial G/\partial a)_\Delta$ is negative or positive. For a fixed $\Delta$, the contact radius corresponding to the minimum of crack speed can be deduced from eqs. (7) and (12), and its value $\|a_i\|$ is the solution of

$$\frac{2\|a\|^4}{\|a_0\|^2 \cdot \|k_m\|^2} + \frac{13\|a\|^3}{3\|a_0\| \cdot k_m\|} + 3\|a\|^2 + \frac{1}{3}\left[\|\Delta\| + \|a_0\|^2 + \frac{2\|P_0\|}{\|a_0\|}\left(1 + \frac{1}{\|k_m\|}\right)\right]\left(1 + \frac{3\|a\|}{\|a_0\| \cdot \|k_m\|}\right) \tag{15}$$

The locus of corresponding points given by eq. (7) with $\|a_c\| = \|a\|$ is plotted in

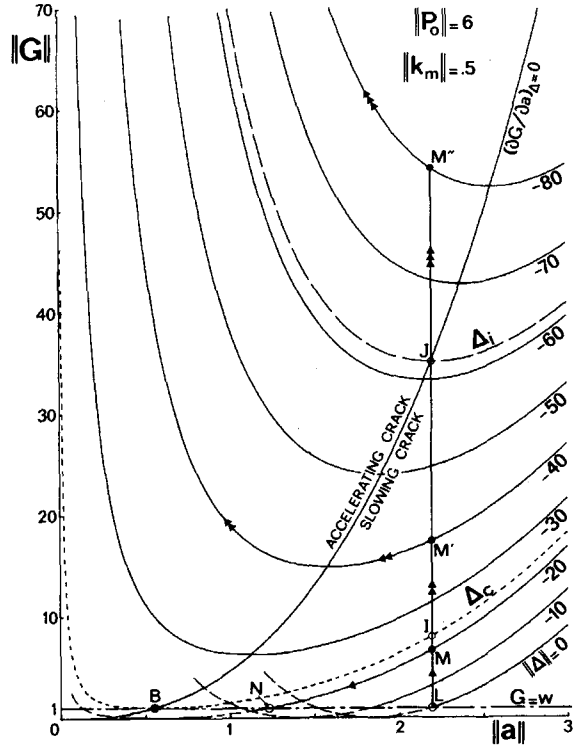


Fig. 3. Strain energy release rate vs. radius of contact area, in reduced coordinates, corresponding to Figure 2.

Figure 2 (branch $OBJ$). So, it is possible to observe a spontaneous increasing crack speed if the fixed displacement $\Delta$ is inferior or equal to the value $\Delta_i$, deduced from eq. (7) with $\|a\| = \|a_0\|$ and eq. (12) with $\|a_c\| = \|a_0\|$:

$$\|\Delta_i\| = -2\|a_0\|^2 \left(\frac{3}{\|k_m\|^2} + \frac{8}{\|k_m\|} + 5\right) \Big/ \left(1 + \frac{3}{\|k_m\|}\right) - \frac{2\|P_0\|}{\|a_0\|}\left(1 + \frac{1}{\|k_m\|}\right) \quad (16)$$

During the propagation along a curve $(\delta)_\Delta$, the kinetics may be studied using eq. (14), the strain energy release rate being given by eq. (3) with $\delta$ calculated by eq. (6). $G$ normalized by $w$ is plotted as a function of contact radius in reduced coordinates in Figure 3. So long as $\Delta$ remains greater than $\Delta_c$ [point $I$, eq. (13)], it is observed that $G$ tends toward the limit $w$ while $a$ decreases toward a new equilibrium value. If $\Delta_i < \Delta < \Delta_c$, with $\Delta_i$ given by eq. (16), $G$ first decreases, then increases: this is reflected by a deceleration followed by an acceleration of the crack and a curve $a(t)$, contact area radius vs. time, has a point of inflexion at radius $a_i$ given by eq. (15). The minimized $G$ is not observed if $\Delta < \Delta_i$ (beyond point $J$); in this case, $G$ increases constantly from its initial value and the crack speed accelerates to rupture.

## EXPERIMENTAL RESULTS AND DISCUSSION

The experiments were carried out using apparatus, shown in Figure 4, consisting essentially of a precision balance supporting at the end of the arm, a

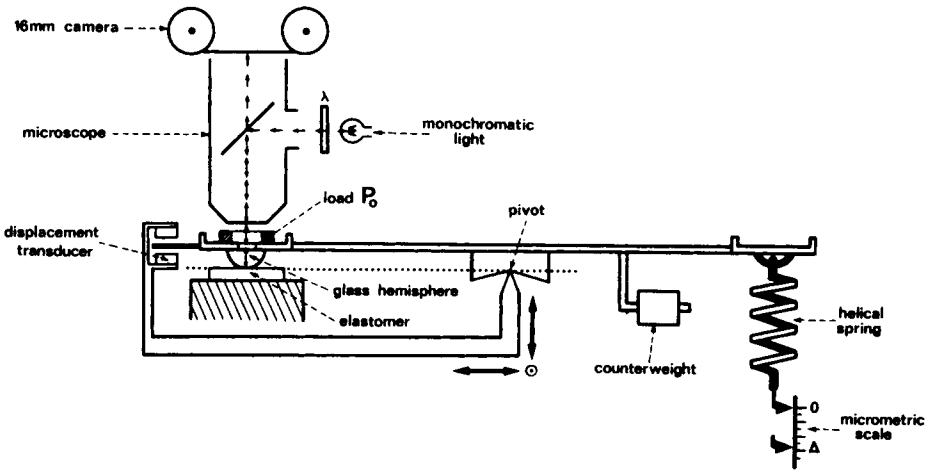


Fig. 4. Schematic arrangement of the apparatus used to study the adherence of a glass hemisphere to viscoelastic materials.

hemispherical glass lens of radius $R = 2.19$ mm. This indenter is applied, for a duration $t_A$, under a compressive load $P_0$, against the flat surface of an elastomer. Then an instantaneous elongation $\Delta$ is imposed to a helical spring of stiffness $k_m$, attached at the other end of the balance arm and linked to a vertical micrometric stage. Five springs with stiffnesses 25.6, 41.9, 57.1, 84.3, and 122.6 $N \cdot m^{-1}$ have been used. The contact area, illuminated by reflection of monochromatic light, is observed through the lens with a microscope. For a quantitative evaluation of the evolution of the contact area during rupture, a 16-mm camera records the contact areas at 25 frames/s with approximately tenfold magnification; the frames were then enlarged and measured. The apparatus also includes an inductive displacement transducer, used to record the displacement $\delta$ of the indenter in the viscoelastic material.

The viscoelastic material chosen was an optically smooth polyurethane, recommended for dynamic studies in photoelasticity (PSM 4 Vishay, $K = 8.9$ MPa) and delivered as plates of thickness $\frac{1}{8}$ in. The surfaces were cleaned with alcohol, dried with warm air, and left during 30 min for the equilibrium with room atmosphere to be reached. Temperature (18.5°C) and relative humidity (62%) remained constant for all the set of experiments. Microscopic examination fails to reveal any surface feature such as exuding substances or dust. The value of Dupré's energy ($w = 61$ mJ/m$^2$) was deduced, by using eq. (1), from initial contact radii measured at the same point on the specimen surface, and, in order to avoid dwell time effects,[14] the contact duration under initial loads was constant ($t_A = 10$ min). In these conditions, the reproducibility is excellent.

Figure 5 shows the variation of the contact radius with time for various stiffnesses and the same displacement $\Delta = -1.6$ mm. For small stiffnesses, a slow return towards a new equilibrium is observed with a continuously decreasing crack speed. The equilibrium being not yet reached after 15 min, the theoretical value of equilibrium radius is noted in Figure 5. As expected, a slowing down of the crack, followed by an acceleration until the rupture is reached, is observed for high stiffnesses. The critical radii of contact $a_i$ given by eq. (15) are reported on the figure, and the agreement with the observed inflexion points is quite good.

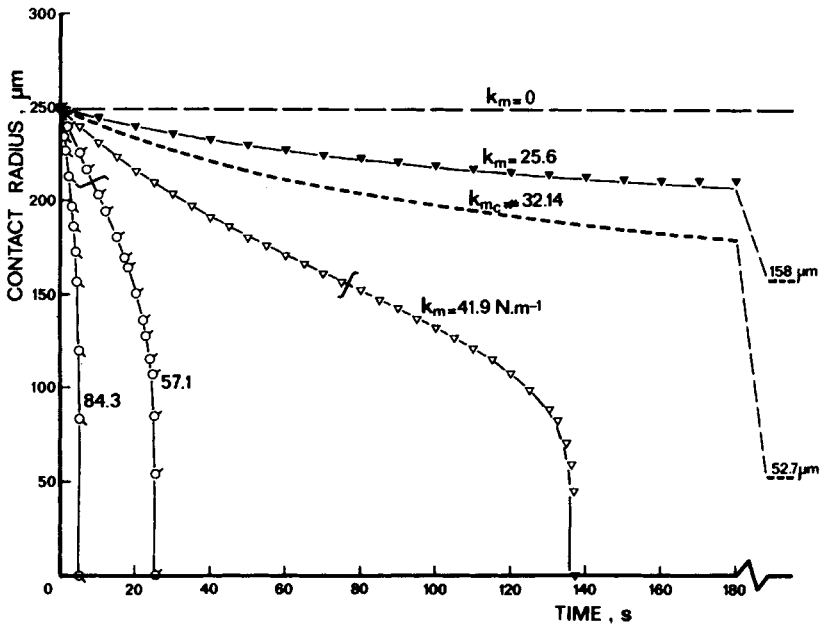


Fig. 5. Variation with time of the radius of contact area of a glass hemisphere in contact with a polyurethane surface, for the same displacement $\Delta$ (−1.6 mm) and various stiffnesses $k_m$.

The dotted curve corresponds to the boundary between the two kinds of evolution of contact area with time; it was computed from eq. (13) and data of Figure 7. For comparison, the dashed line ($k_m = 0$) represents the case of an unloading at constant load, and the $a$-axis, an unloading at fixed grips condition ($k_m = \infty$).

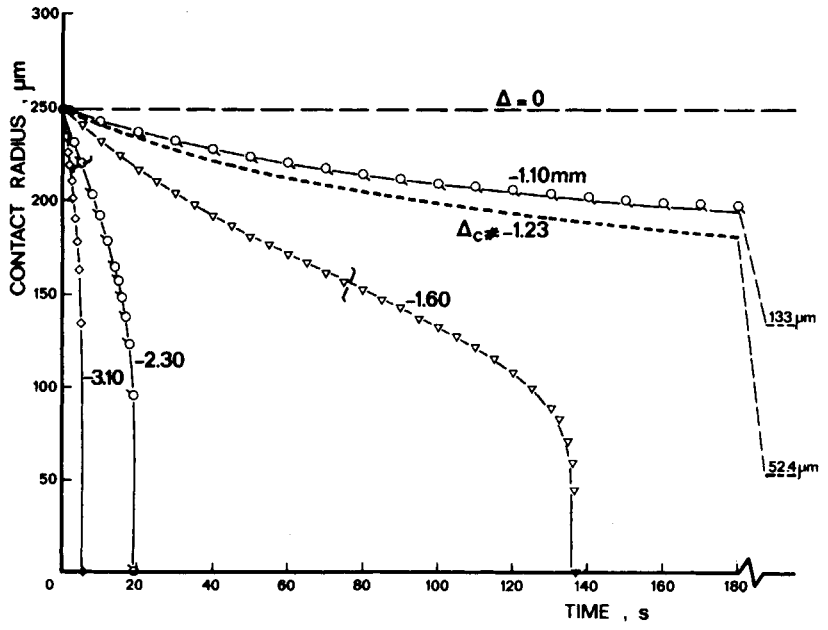


Fig. 6. Variation with time of the radius of contact area of a glass hemisphere in contact with a polyurethane surface, for the same stiffness $k_m$ (41.9 N·m$^{-1}$) and various displacements $\Delta$.

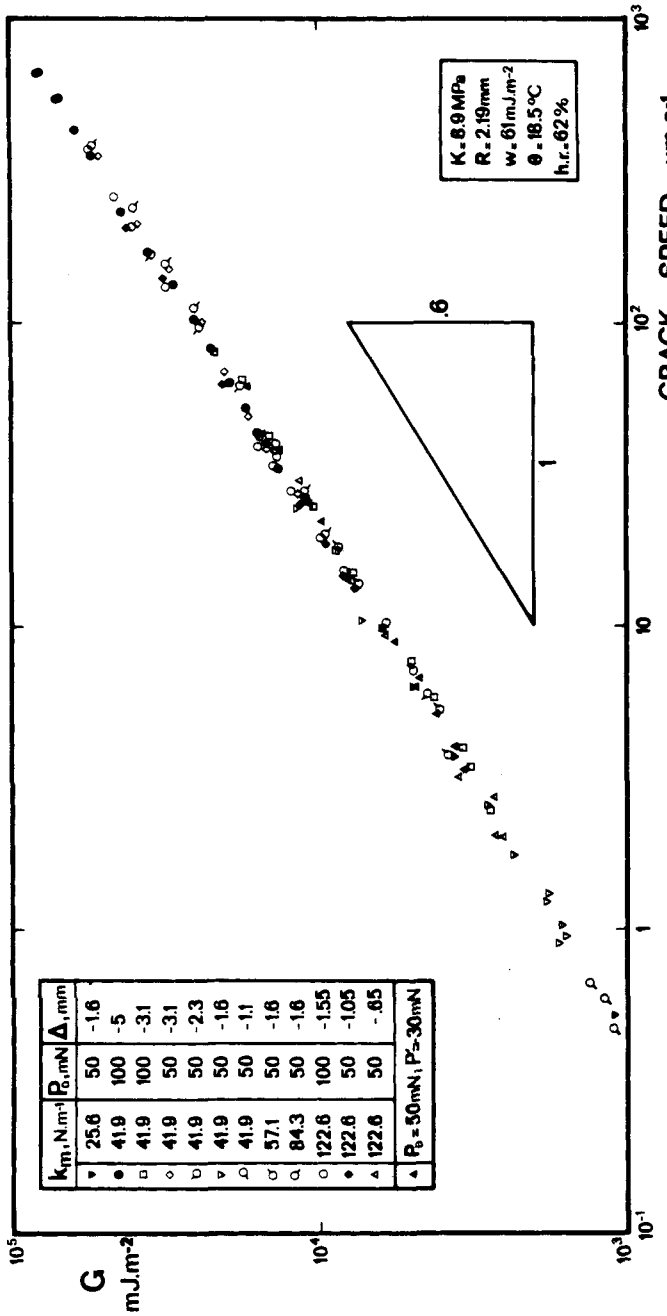


Fig. 7. Relation between strain energy release rate $\dot{G}$ and crack speed $v = da/dt$, for different tests with various stiffnesses, initial loads and displacements $\Delta$: $K = 8.9$ MPa; $R = 2.19$ mm; $W = 61$ mJ·m$^{-2}$; $\theta = 18.5$°C; hr = 62%.

Thus, Figure 5 clearly shows the influence of machine stiffness on the kinetics of adherence of an elastomer.

Figure 6 displays the variation of contact radius with time for various displacements $\Delta$ and the same helical spring of stiffness $k_m = 41.9$ N·m$^{-1}$. A similar behavior as in Figure 5 is observed: a small $\Delta$ leads to a new equilibrium with a constantly decreasing speed of propagation, and a large $\Delta$ provokes first a decreasing crack speed and then an accelerating crack speed until contact is completely broken. Moreover, observed inflexion points are in good agreement with theoretical values deduced from eq. (15). As expected, for a very large $\Delta$, an instantaneous increasing crack speed is observed. The dotted line, computed from data of Figure 7, represents the evolution of contact area with time for the critical displacement $\Delta_c = -1.23$ mm, corresponding to the limit of stability [eq. (13)].

Rupture of equilibrium for various stiffnesses $k_m$, initial loads $P_0$, and displacements $\Delta$ are shown in a diagram $G(v)$ on Figure 7: the strain energy release rate $G$ is calculated by eq. (3) with $\delta$ given by eq. (6), and the crack speed is deduced from the slope at each of the points of a curve $a(t)$. All the results corroborate the previous findings[4] and consequently confirm the general equation $G - w = w\phi(a_T v)$ [eq. (14)], in which the function $\phi$ for polyurethane specimen varies[4,12–14] as the sixth power of $v$, with $w = 61$ mJ·m$^{-2}$. For comparison, results of unloading from $P_0 = 50$ mN to $P' = -30$ mN (i.e., at $k_m = 0$), realized in the same condition of temperature and relative humidity, are given in Figure 7: experimental points fall on the same curve.

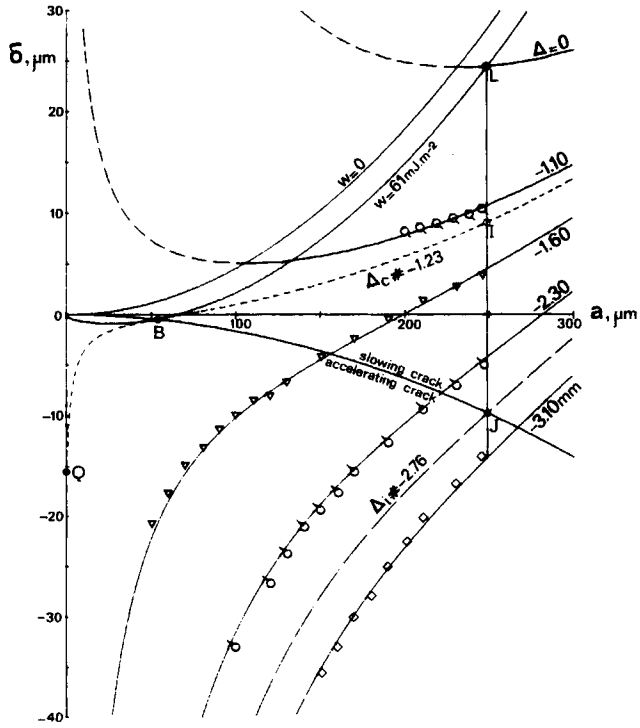


Fig. 8. Displacement $\delta$ vs. radius of contact area $a$ corresponding to Figure 6: $K = 8.9$ MPa; $R = 2.19$ mm; $P_0 = 50$ mN; $k_m = 4.19$ N·m$^{-1}$.

By numerical integration of the general equation [eq. (14)], taking into account eqs. (3) and (6) and the variation of $\phi$ with the sixth power of $v$, it is possible to predict the results of Figures 5 and 6. Computed curves (light lines) are in good agreement with experimental data: the light divergence observed for long times is probably due to dwell time effect resulting from the relaxation of stresses stored in the roughnesses compressed during initial contact.[14]

Elastic displacements $\delta$ have been recorded during crack propagation. Figure 8 gives results corresponding to experiments described in Figure 6. The agreement with theoretical prediction (Fig. 2) is excellent: the purely elastic character of the displacements $\delta$ is clearly apparent, and it is shown that viscoelastic losses are strictly limited to the crack tip.

## CONCLUSION

It is shown that the introduction of the fracture mechanics concepts, such as the strain energy release rate $G$, to solve the problem of the adherence of elastomers, the edge of contact being regarded as a crack propagating in mode I in the interface, allows one to predict the dependence of the adherence force with the stiffness of testing machines.

It has been shown that the general equation of the kinetics of adherence proposed earlier,[4] $G - w = w\phi(a_T v)$, where $w$ is Dupré's work of adhesion and $\phi$ a dissipation function characteristic of the material, is confirmed whatever the stiffness of the testing machine and the instantaneous deformation imposed. Experiments realized with a hemispherical glass lens in contact on a polyurethane surface verify theoretical predictions with an accuracy better than 1%.

The author would like to express his gratitude to the Direction des Recherches, Etudes et Techniques, for the financial support given to this work (DRET Contract No. 78-609).

## References

1. K. L. Johnson, K. Kendall, and A. D. Roberts, *Proc. Roy. Soc. London A*, **324,** 301 (1971).
2. K. Kendall, *J. Phys. D. Appl. Phys.*, **4,** 1186 (1971).
3. D. Maugis, M. Barquins, and R. Courtel, *Mét. Corros. Ind.*, **605,** 1 (1976).
4. D. Maugis and M. Barquins, *J. Phys. D. Appl. Phys.*, **11,** 1989 (1978).
5. D. Maugis and M. Barquins, in *Adhesion and Adsorption of Polymers*, L. H. Lee, Ed., Plenum, New York, 1980, Vol. 12A, pp. 203–277.
6. R. Courtel, D. Maugis, and M. Barquins, *Ind. Min., n° Spéc. Rhéol.*, **4,** 137 (1977).
7. M. Barquins, *Int. J. Adhesion Adhesives*, **3,** 71 (1983).
8. M. Barquins and D. Maugis, *J. Adhesion*, **13,** 53 (1981).
9. M. Barquins and D. Maugis, *J. Mec. Theor. Appl.*, **1,** 331 (1982).
10. A. N. Gent and J. Schultz, *J. Adhesion*, **3,** 281 (1972).
11. E. H. Andrews and A. J. Kinloch, *Proc. Roy. Soc. London A*, **332,** 385 (1973).
12. M. Barquins, "Etude théorique et expérimentale de la cinétique de l'adhérence des élastomères," thesis, University of Paris, 1980.
13. A. D. Roberts, *Rubber Chem. Techn.*, **32,** 23 (1979).
14. M. Barquins, *J. Adhesion*, **14,** 63 (1982).

Received February 2, 1983
Accepted March 28, 1983